A&A manuscript no.
(will be inserted by hand later)

Your thesaurus codes are:
08.16.4, 08.13.2, 13.09.6, 09.16.1, 09.04.1

ASTRONOMY
AND
ASTROPHYSICS
23.8.1996

Mineralogy of Oxygen-rich dust shells*

L.B.F.M. Waters[1,2], F.J. Molster[1], T. de Jong[2,1], D.A. Beintema[2], C. Waelkens[3], A.C.A. Boogert[8], D.R. Boxhoorn[2], Th. de Graauw[2], S. Drapatz[9], H. Feuchtgruber[9], R. Genzel[9], F.P. Helmich[10], A.M. Heras[4], R. Huygen[3], H. Izumiura[7], K. Justtanont[2], D.J.M. Kester[2], D. Kunze[9], F. Lahuis[4], H.J.G.L.M. Lamers[2], K.J. Leech[4], C. Loup[6], D. Lutz[9], P.W. Morris[4], S.D. Price[12], P.R. Roelfsema[2], A. Salama[4], S.G. Schaeidt[9], A.G.G.M. Tielens[11], N.R. Trams[4], E.A. Valentijn[2], B. Vandenbussche[3], M.E. van den Ancker[1], E.F. van Dishoeck[10], H. van Winckel[3], P.R. Wesselius[2], and E.T. Young[13]

[1] Astronomical Institute 'Anton Pannekoek', University of Amsterdam, Kruislaan 403, NL-1098 SJ Amsterdam, the Netherlands
[2] SRON Laboratory for Space Research Groningen, P.O. Box 800, NL-9700 AV Groningen, The Netherlands
[3] Instituut voor Sterrenkunde, Katholieke Universiteit Leuven, Celestijnenlaan 200B, B-3001 Heverlee, Belgium
[4] ESA Villafranca, P.O. Box 50727, E-28080 Madrid, Spain,
[5] SRON Laboratory for Space Research Utrecht, Sorbonnelaan 2, 3584 CA Utrecht, the Netherlands
[6] Institut d'astrophysique de Paris, 98bis Boulevard Arago, F-75014 Paris, France
[7] Department of Astronomy and Earth Sciences, Tokyo Gakugei University, Konagei, Tokyo 184, Japan
[8] Kapteyn Astronomical Institute, P.O. Box 800, NL-9700 AV Groningen, The Netherlands
[9] Max-Planck-Institut Für Extraterrestrische Physik, Postfach 1603, D-85740 Garching, Germany
[10] Leiden Observatory, P.O. Box 9513, 2300 RA Leiden, The Netherlands
[11] NASA Ames Research Center, Mail Stop 245-6, Moffett Field, CA 94035, U.S.A.
[12] Geophysics Directorate, Phillips Laboratory, 29 Randolph Rd., Hanscom AFB, MA01731-3010, U.S.A.
[13] Steward Observatory, University of Arizona, Tucson, AZ 85721, U.S.A.

received date; accepted date

Abstract. Spectra taken with the Short Wavelength Spectrometer on board of the Infrared Space Observatory of dust shells around evolved oxygen-rich stars reveal the presence of several emission features at wavelengths between 20 and 45 μm. These features have a range of widths and strengths, but are all narrow compared to the well-known amorphous silicate bands at 9.7 and 18 μm. The emission peaks are tentatively identified with crystalline forms of silicates such as pyroxenes and olivine. The emission features tend to be more prominent for objects with cooler dust shells (T $<$ 300 K). This may be due to an intrinsic change in optical properties of the dust as it cools, or it may be due to an increase in the fraction of crystalline silicates compared to amorphous forms as the mass loss rate increases. The implications for the physics of dust formation in the outflows of cool giants are briefly discussed.

Key words: Infrared: stars - Stars: AGB and post-AGB; mass loss - Planetary Nebulae - Dust

1. Introduction

The late stages of evolution of low and high mass stars are characterized by strong stellar winds, in which the conditions are favourable for the formation of dust grains. These dust grains efficiently absorb the optical and UV radiation of the central star, and re-emit this radiation at IR wavelengths, thus shifting the peak of the energy distribution to longer wavelengths.

It is believed that stellar pulsations in combination with dust formation play an important role in driving the mass loss. However, current understanding of the physical processes that take place in the extended atmospheres of Asymptotic Giant Branch (AGB) stars and in Red Supergiant (RSG) stars is still limited. In particular the grain nucleation process is difficult to model from first principles, and existing models lack observational data to constrain model parameters.

The Short Wavelength Spectrometer (SWS) on board of the Infrared Space Observatory (ISO) is ideally suited to study the composition of dusty envelopes surrounding evolved stars. For a description of the instrument and its main features we refer to de Graauw et al. (this volume) and to Kessler et al. (this volume). In this paper we report on first results of the SWS guaranteed time programmes on RSG, AGB stars, post-AGB stars and Planetary Nebulae (PNe). We concentrate on O-rich envelopes of representative cases, and show that the 12-45 μm part of the spectrum is rich in structure. We tentatively identify these structures with crystalline forms of silicates such as olivine and

Send offprint requests to: L.B.F.M. Waters (Amsterdam address)

* Based on observations with ISO, an ESA project with instruments funded by ESA Member States (especially the PI countries: France Germany, the Netherlands and the United Kingdom) and with the participation of ISAS and NASA

pyroxenes. The dust features seem to occur preferentially in dust shells with a low colour temperature ($\sim$ 300 K or less). A feature at 11.3 μm attributed to crystalline olivine has been observed in the spectra of comets (Hanner et al. 1994; Herter et al. 1987), and in several Vega stars (e.g. Fajardo-Acosta et al 1993; Knacke et al. 1993).

Table 1. Observing log.

Name	type	AOT01 speed	Date
W Hya	AGB	2	14-02-96
NML Cyg	RSG	4	09-01-96
AFGL4106	P-AGB	2	29-02-96
HD179821	P-AGB	2	09-03-96
NGC6302	PN	4	19-02-96
NGC6543	PN	4	12-12-95

2. The observations

We selected from the guaranteed time observing programme 6 representative cases, two mass-losing objects (a RSG and an AGB star), two post-AGB stars and two PNe (Table 1). The observations were carried out using the SWS AOT01 full scan observing mode, at speeds 2 and 4. Table 1 lists the observing log. The spectra were reduced using standard procedures. The data were inspected for cosmic ray hits which were removed by hand. Dark subtraction was done using a linear fit to the dark measurements taken during the observation. The absolute flux calibration was obtained using the calibration files in version 4.1 of the ISO-SWS off-line processing pipeline. We estimate that the flux calibration in the 30-45 μm region is accurate to 30-50 percent (Schaeidt et al. 1996). In this paper we concentrate on the 30-45 μm part of the scans, corresponding to band 4 of the SWS. The spectra are plotted in Figure 1, where we rebinned the data to a resolution of 300 ($\lambda/\Delta\lambda$). Note that the intrinsic resolution of the spectrograph is significantly better than 300 (see de Graauw et al. 1996). Due to the rebinning procedure the 30-45 μm spectrum of W Hya and NML Cyg do not show the emission lines due rotational transitions of H_2O reported by Neufeld et al. (1996) and Justannont et al. (1996a). We postpone a full discussion of the spectra to a later paper. We show in Figure 1 the individual data points as well as a weighted average. The dotted line in the top left panel of Fig. 1 shows the shape of the relative spectral response curve used to divide out instrumental effects. Although this curve shows structure near wavelengths where we find some of the bumps in the programme stars, we also find many objects that are featureless (such as W Hya) using the same response function; we conclude that the bumps we report here are real.

3. Discussion

The six programme stars discussed in this *Letter* are all oxygen-rich, as evidenced from the occurrence of OH maser emission, or from the molecular bands seen in the optical or near-IR. Also in several objects (W Hya, NML Cyg, AFGL 4106, HD 179821) the 9.7 μm silicate band (not shown here) is seen either in emission or absorption, pointing to an O-rich chemistry in the shell. The programme stars show a remarkably rich spectrum between 30 and 45 μm, with several bumps with a variety in strength and shape. Also, in several objects we find a plateau between 31 and 36-37 μm. W Hya however shows an almost featureless spectrum (apart from the water lines). Table 2 gives a summary of the bumps with their wavelength and line over continuum ratio. In Fig. 1 we have indicated the position of the strongest features with tick marks in the upper panels.

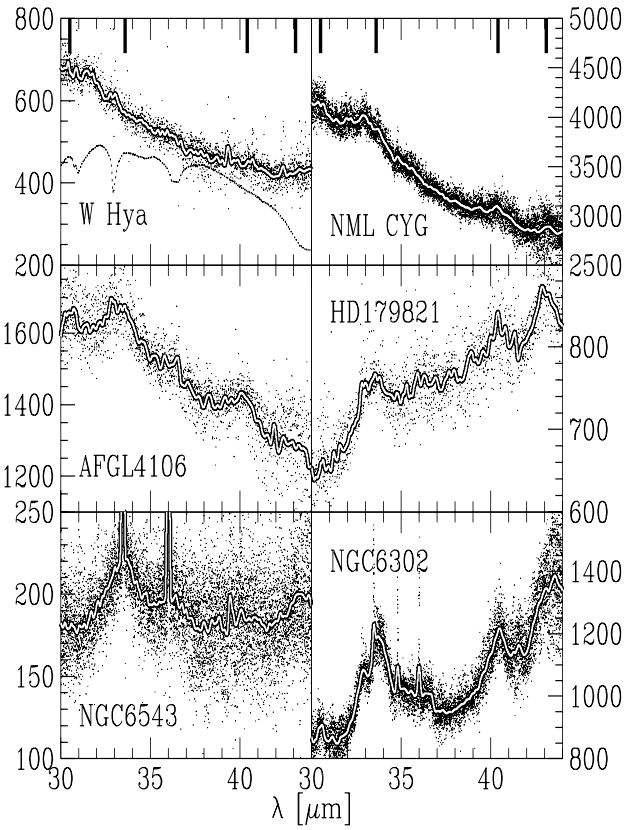

Fig. 1. SWS 30-45 μm spectra of the programme stars (Table 1). Flux is in Jy

The bumps are strongest in the post-AGB stars and PNe, while they are weak in NML Cyg and virtually absent in W Hya. This suggests that the appearance of the bumps is somehow related to the colour temperature of the dust shell, the bumps being absent in 'warm' dust shells, while they are prominent in dust shells with colour temperature less than about 300 K. Inspection of the spectra of other stars observed with SWS shows a similar trend. In mass-losing RSG or AGB stars the colour temperature of the dust is a measure of the mass loss rate of the star, while in post-AGB stars and PNe it is a measure of the time which has passed since the star left the AGB. This suggests a relation between the occurrence of the

bumps either with grain formation conditions (high mass loss versus low mass loss) or with age and temperature (post-AGB and PNe; see also below).

The width and shape of the bumps, which are all resolved at a resolution of 300, suggest that they are due to vibrational or bending modes in solid state material (grains). We have tried to identify the carriers of the bumps by comparing published laboratory spectra of O-rich grain material (silicates, oxides) to the observed spectra. It is clear from these (preliminary) comparisons that we are dealing with a *mixture* of materials, i.e. no single component that we are aware of can fit the observed spectra. This may not be surprising since the relative strength of some bumps seems to correlate while others do not, also pointing to a mixture of carriers.

Table 2. wavelength and possible identification of features

Name	λ μm	FWHM μm	I_p/I_c	flux W/m^2 $*10^{-14}$	ident
W Hya	31.7 $\pm$ 0.1	0.9	1.06	9.0	u
NML Cyg	30.5 $\pm$ 0.1	0.6	1.02	20	u
	32.95 $\pm$ 0.01	0.83	1.06	71	f?
	33.75 $\pm$ 0.01	0.59	1.05	35	o
	40.40 $\pm$ 0.03	1.2	1.05	37	cp
	43.19 $\pm$ 0.04	0.61	1.026	7	i
AFGL4106	30.52 $\pm$ 0.03	0.8	1.04	18	u
	32.83 $\pm$ 0.01	0.4	1.06	23	f?
	33.50 $\pm$ 0.03	1.0	1.06	16	o
	36.51 $\pm$ 0.02	0.4	1.04	6	u
	40.1 $\pm$ 0.1	1.6	1.07	27	cp
	43.0 $\pm$ 0.2	1.4	1.04	13	i
HD179821	30.59 $\pm$ 0.01	0.28	1.028	2	u
	32.82 $\pm$ 0.01	0.4	1.08[2]	5	f?
	33.49 $\pm$ 0.01	1.0	1.08[2]	12	o
	31.7-37.1 $\pm$ 0.3			23	plateau[1]
	40.39 $\pm$ 0.01	0.8	1.06	7	cp
	43.1 $\pm$ 0.1	1.24	1.08	15	i
NGC6302	30.52 $\pm$ 0.04	0.35	1.06	8	u
	32.80 $\pm$ 0.02	0.5	1.15[2]	60	f?
	33.70 $\pm$ 0.01	0.95	1.21[2]	19	o
	31.7-37.2 $\pm$ 0.2			72	plateau[1]
	40.46 $\pm$ 0.05	1.10	1.15	31	cp
	41.54 $\pm$ 0.02	0.34	1.045	3.5	u
	43.1 $\pm$ 0.1	1.51	1.10	30	i
NGC6543	31.4-37.5 $\pm$ 0.3			22	plateau[1]
	33.38 $\pm$ 0.03	1.6	1.12[2]	11	o
	43.34 $\pm$ 0.04	1.22	1.08	3.0	i

notes to table 2: o = crystalline olivine; cp = clino-pyroxene; f = forsterite; i = crystalline ice; u = unidentified. [1] plateau is unidentified; [2] $I_p/(I_c$ + plateau)

The most promising candidates for the carriers of the bumps are crystalline silicates, such as Olivine and Pyroxenes, with various mixtures of Fe and Mg (e.g. Jäger et al. 1994; Koike et al. 1993). We have indicated possible identifications in Table 2. Amorphous materials do not show prominent structure beyond 20 μm (e.g. Jäger et al. 1994). We point out however that the 10 μm spectrum of NML Cyg has a shape which fits amorphous silicates, which suggests that at least in that object there is a significant amount of amorphous material present. This may also be the case for the other objects (see e.g. Guertler et al. 1996). We conclude that the dust shells of our programme stars consist of a mixture of amorphous and crystalline silicates. Crystalline olivine shows peaks at 11.3 and 23.8-25.9 μm in addition to a peak at 33.8 μm (Koike et al 1993). A 23.5 μm peak is seen in AFGL 4106, HD 179821, NGC6543, NGC6302 and possibly in NML Cyg, but not in W Hya, which is close to that expected for olivine. The spectra of several objects show structure around 11.3 μm, i.e. where emission from crystalline silicates is expected. However this may be instrumental and not intrinsic. In Figure 2, we show the extinction curves for several materials that were measured in the lab by Koike et al. (1993).

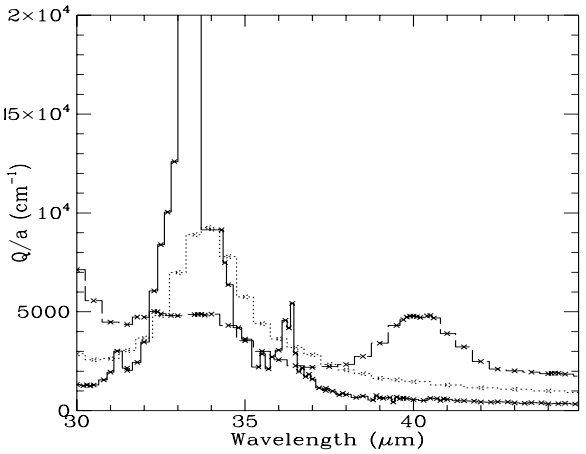

Fig. 2. Laboratory spectra of crystalline silicates, taken from Koike et al. (1993). Solid line: forsterite; Dotted line: olivine; Dashed line: clino-pyroxene.

We also considered the possibility that the bumps are due to metal oxides, such as Al_2O_3, and Fe-Mg oxides. Evidence for the occurrence of oxides in oxygen-rich dust envelopes is growing. The LRS spectra of some Mira variables with a broad peak between 12 and 13 μm were interpreted by Vardya et al. (1986) as due to grains containing aluminum oxide. Interestingly, the occurrence of the 12-13 μm peaks seems to be related to the shape of the optical light curve, suggesting a relation between the physical conditions in the dust-forming region and the kind of dust that condensates (Onaka et al . 1989) From a re-classification of IRAS LRS spectra Goebel et al. (1989) find a class of objects with bumps at 11+, 13.1 and 19 μm, which they interpret as due to metal oxides. Henning et al. (1995) publish new optical constants for Mg-Fe oxides and find that these materials show structure in the 15-24 μm wavelength region. It

is possible that metal oxides contribute to the bump seen at 23.5 μm. However, we are not aware of laboratory measurements of oxides that show structure between 30 and 45 μm. We point out that the list of spectral features presented in this *Letter* is preliminary and certainly not complete for wavelengths shortward of 30 μm. For example, NML Cyg shows a bump near 20 μm which could be due to oxides.

A third possibility for the origin of the bumps are (crystalline) ices. Emission from ice in the 40-70 μm spectrum of the 'Frosty Leo' and other cool oxygen-rich envelopes was reported by Omont et al. (1990). Laboratory spectra of crystalline H_2O ices show a narrow emission at 44 μm (Bertie et al. 1969) as well as a broader feature at 62 μm. Indeed one of the features we find peaks near 43 μm (Table 2). We have tentatively identified the 43 μm bump with crystalline ice. Confirmation of this identification may come from LWS spectra which then should show the 62 μm feature.

If the identification of the bumps with crystalline material is correct, the correlation with dust temperature seems puzzling. It is believed that silicates condense in dusty outflows with amorphous structure, as evidenced by the ubiquitous broad and smooth appearance of the 9.7 and 18 μm silicate bumps (e.g. Bedijn 1987). Conversion of this material to crystalline forms requires restructuring of the lattice which can be done by heating the grains. However, heating of dust grains is not expected to occur in the post-AGB phase and indeed is not observed. Rather, cooling of the dust shell as it expands is observed. It is important to realise however that dust in post-AGB stars represents a final burst of very high mass loss (10^{-5} to 10^{-4} $M_\odot$/yr) and so the conditions in the dust forming region during this very high mass loss phase may have been similar to that seen in the reddest AGB stars or RSG we observe now. Indeed, NML Cyg, the reddest mass-losing object in our sample, shows the bumps in emission. Therefore it is possible that the conditions in the dust forming regions of AGB stars and RSGs with extreme mass loss rates and high wind densities allow the formation of crystalline silicates. This could occur if the grains stay warm in this high-density region for a relatively long period of time, i.e. do not cool rapidly after formation.

It is also possible that the intrinsic properties of the dust grains change with temperature. There is some evidence from model fitting of cool oxygen-rich dust shells that the strength of the 18 μm bending mode of SiO increases with decreasing temperature (Bedijn 1987; Justtanont et al. 1996b). Note that the observed ratio of the 18 to 9.7 μm silicate features depends on the temperature of the dust shell as well as on the optical constants (see e.g. Ossenkopf et al. 1992). It is not clear however how important this effect is for the 30-45 μm features.

It is interesting to point out that bumps similar to the ones reported here have also been found in cool dust shells surrounding LBV's (Lamers et al., this volume) and in young Herbig Ae/Be stars (Waelkens et al., this volume). All these objects are believed to be oxygen-rich. Prior to ISO, structure in the 30 μm spectra of O-rich stars was, to our knowledge, not reported. However the 23.5 μm feature was previously found in spectra of comet Halley (Herter et al. 1987) and was identified with crystalline olivine.

The dust features reported in this paper can be added to the growing list of structures found in spectra of oxygen-rich stars. Goebel et al. (1994) report on the discovery of 7.15 μm emission in O-rich shells, and they also list features at 10, 13.1, 18 and 19.7 μm. These features are attributed to metal oxides. It is clear that these new observations force us to revise the picture of a standard mix of silicates ('astronomical silicates', e.g. Draine & Lee 1984). The full wavelength coverage of the SWS and LWS spectrographs allow us to make a much more detailed inventory of the composition of dust shells in evolved stars, i.e. to perform mineralogy of these objects.

Acknowledgements. It is a pleasure to thank Drs. Koike, Dorschner, Henning and Lynch for sending us information on laboratory spectra of silicates and oxides, and Dr. Henning for critically reading the manuscript. LBFMW acknowledges financial support from the Royal Netherlands Academy of Arts and Sciences, and from an NWO 'Pionier' grant. FJM acknowledges support from NWO grant 781-71-052.

References

Bedijn, P.J.: 1987, A&A 186, 136
Bertie, J.E., Labbe, H.J., Whalley, E.: 1969, J. Phys. Chem. 50, 4501
de Graauw, Th., et al.: 1996, (this issue)
Draine, B.T., Lee, H.M.: 1984, ApJ 285, 89
Fajardo-Acosta, S.B., Telesco, C.M., Knacke, R.F.: 1993, ApJ 417, L33
Goebel, J., Volk, K., Walker, H.J., Gerbault, F., Cheeseman, P., Self, M., Stutz, J., Taylor, W.: 1989, A&A 222, L5
Goebel, J.H., Bregman,J.D., Witteborn, F.C.: 1994, apJ 430, 317
Guertler, J., Koempe, C., Henning, T.: 1996, A&A 305, 878
Hanner, M.S., Lynch, D.K., Russell, R.W.: 1994, ApJ 425, 274
Henning, Th., Begemann, B., Mutschke, H., Dorschner, J.: 1995, A&AS 112, 143
Herter, T., Campins, H., Gull, H.E.: 1987 A&A 187, 629
Jäger, C., Mutschke, H., Begemann, B., Dorschner, J., Henning, Th.: 1994, A&A 292, 641
Justtanont, K., et al.: 1996a (this issue)
Justtanont, K., Skinner, C.J., Tielens, A.G.G.M., Meixner, M., Baas, F.: 1996b, ApJ 456, 337
Kessler, M.F., et al., 1996 (this issue)
Koike, C., Shibai, H., Tuchiyama, A.: 1993, MNRAS 264, 654
Neufeld, D.A. et al.: 1996, (this issue)
Omont, A., Forveille, t., Moseley, S.H., Glaccum, W.J., Harvey, P.M., Likkel, L., Loewenstein, R.F., Lisse, C.M.: 1990, ApJ 355, L27
Onaka, T., de Jong, T., Willems, F.J.: 1989, A&A 218, 169
Ossenkopf, V., Henning, Th., Mathis, J.S.: 1992, A&A 261, 567
Schaeidt, S. et al., 1996 (this issue)
Vardya, M.S., de Jong, T., Willems, F.J.: 1986, ApJ 304, L29
Waelkens, C., et al., 1996 (this issue)

This article was processed by the author using Springer-Verlag LaTeX A&A style file *L-AA* version 3.